HHS Public Access

Author manuscript

J Biomed Mater Res B Appl Biomater. Author manuscript; available in PMC 2020 July 19.

Published in final edited form as:

J Biomed Mater Res B Appl Biomater. 2019 August ; 107(6): 1864–1876. doi:10.1002/jbm.b.34279.

Woven collagen biotextiles enable mechanically functional rotator cuff tendon regeneration during repair of segmental tendon defects *in vivo*

Greg D. Learn[1,†], **Phillip E. McClellan**[2,†], **Derrick M. Knapik**[3], **Jameson L. Cumsky**[4], **Victoria Webster-Wood**[2], **James M. Anderson**[1,5,6], **Robert J. Gillespie**[3], **Ozan Akkus**[1,2,3]

[1]Department of Biomedical Engineering, Case Western Reserve University, Cleveland, Ohio

[2]Department of Mechanical and Aerospace Engineering, Case Western Reserve University, Cleveland, Ohio

[3]Department of Orthopaedic Surgery, University Hospitals of Cleveland, Cleveland, Ohio

[4]School of Medicine, Case Western Reserve University, Cleveland, Ohio

[5]Department of Pathology, Case Western Reserve University, Cleveland, Ohio

[6]Department of Macromolecular Science, Case Western Reserve University, Cleveland, Ohio

Abstract

Despite advancements in surgical techniques and materials for rotator cuff repair procedures, primary repair failures remain common. This study examines the use of electrochemically aligned collagen (ELAC) threads woven into biotextile scaffolds as grafts to repair critical infraspinatus tendon defects in New Zealand White rabbits. Three surgical treatment groups were evaluated: rabbits undergoing direct repair as operative controls, rabbits receiving ELAC scaffolds alone, and rabbits treated with mesenchymal stem cell (MSC)-seeded ELAC scaffolds. In each animal, the intact, contralateral infraspinatus served as an internal positive control. Tendon–bone constructs were harvested after 3 months *in vivo* and outcome measures included biomechanical testing, histological staining, and immunohistochemical staining. Biomechanical testing revealed that maximum load-bearing capacity was comparable between all groups, while MSC-seeded scaffold repairs exhibited increased stiffness relative to non-seeded scaffold repairs. Histological staining revealed robust collagen deposition around ELAC fibers and increased cellularity within the continuum of woven scaffolds as compared to native tendon. Immunohistochemical staining revealed presence of collagens I and III in all groups, but procollagen I and the tendon-specific marker tenomodulin were only observed in seeded and non-seeded ELAC scaffold repairs. Findings of this pilot study warrant continued investigation of ELAC biotextile scaffolds for repair of critically-sized rotator cuff tendon defects.

Correspondence to: O. Akkus; oxa@case.edu.

†Contributed equally to this work.

Additional Supporting Information may be found in the online version of this article.

Keywords

rotator cuff; collagen; tendon; tissue engineering; biomaterial

INTRODUCTION

Tendon injuries are a common source of pain and disability, and surgical intervention is often recommended to repair injured tendons due to their limited intrinsic healing capacity. Unfortunately, primary operative repair failures are prevalent, especially with regard to rotator cuff tendons.[1] Direct costs associated with the ~300,000 rotator cuff repair procedures performed in the United States each year are estimated to range between $3 and $12 billion.[2,3] One in every four rotator cuff repairs suffers a recurrent tear,[3] with tear size and the extent of soft tissue degeneration prior to the initial repair surgery being the leading risk factors associated with re-tears.[3,4] As tear size increases, the tension required to restore anatomical tendon contact at the original site of insertion becomes greater. The combination of increased tension and poor suture retention properties inherent in the aligned tendon matrix leads to increased susceptibility of the tendon to separate from bone, precluding successful tendon-to-bone healing. As a consequence, repairs of full-thickness rotator cuff tears classified as large or massive fail on a regular basis and require revision surgery. Moreover, soft tissue degeneration is prevalent following rotator cuff tendon repair, occurring predominantly by way of fatty infiltration of the injured tendon and associated musculature, further impairing restoration of normal biomechanical function and resulting in inferior functional outcomes.[4–6] As such, repairs of large to massive rotator cuff tendon tears remain suboptimal, despite continued advancements in surgical techniques and instrumentation.[7]

Given the need for more effective treatment approaches to restore function to damaged tendons, many biomaterials, engineered tissue replacements, and biologics are under active investigation. Experimental strategies to promote tendon healing that are currently being explored include the use of decellularized matrices,[8–11] biodegradable polymer scaffolds,[11–15] growth factor administration,[16] genetic reprogramming,[17–20] and mechanical stimulation.[21,22]. However, despite decades of basic and clinical science research on tendon repair, there is no clear consensus regarding an approach to improve clinical success in repairs of large or massive rotator cuff tears.

One biomimetic strategy that holds unique potential to regenerate and restore function of torn tendons involves the fabrication of tissue engineering constructs composed of collagen, a biopolymer comprising 90% of the extracellular matrix (ECM) in native tendon. The main limitation exhibited by reconstituted collagen biomaterials (e.g., collagen gels or sponges) in the repair of tendon to date has been insufficient mechanical strength.[23–25] This limitation may be overcome by utilizing a biofabrication process known as electrocompaction, which assembles fibers of aligned collagen molecules from solution.[26] Using this technique, electrochemically aligned collagen (ELAC) threads possessing exceptional mechanical robustness and favorable bioinductive properties can be generated.[27–30] ELAC threads inserted into a partial defect created within the patellar tendon of rabbits and highlighted a

lack of severe immune response, no ectopic bone formation, and degradation times of up to 8 months *in vivo*.[27] Textile scaffolds woven from chemically cross-linked ELAC threads have exhibited mechanical properties comparable to those of the native infraspinatus tendon in rabbits.[28] Additionally, as they are precursors to tendon (among several musculoskeletal tissues) commonly applied in tendon tissue engineering,[31,32] mesenchymal stem cells (MSCs) cultured on woven ELAC scaffolds in the absence of exogenous growth factors have displayed genetic markers and proteins associated with tenogenic differentiation.[28,30] The tenoinductive properties of ELAC threads are attributed to the influence of topographic cues conveyed by the dense and aligned collagen substrate.

These prior data demonstrating mechanical robustness and tenoinductivity of ELAC *in vitro* and *in vivo* motivated a preliminary assessment of ELAC performance with respect to functional repair and regeneration of segmental tendon defects *in vivo* in the present study. A pilot investigation with a small number of animals was conducted using an animal model of an irreparable infraspinatus tendon defect in New Zealand White rabbits. Repairs of critically-sized gap defects using ELAC biotextiles or ELAC biotextiles seeded with marrow-derived, allogeneic MSCs were compared to a clinical standard, direct repair technique. The goals of this study were as follows: (1) to establish an *in vivo* surgical model in rabbits for rotator cuff injury and repair with ELAC biomaterial, (2) to preliminarily assess the potential efficacy of ELAC when used as a graft to replace or regenerate a substantial volume of tendon tissue, and (3) to explore the synergy of ELAC biomaterial and MSCs. Our hypotheses were: ELAC biotextiles retain their mechanical robustness following 3 months of functional loading in a critically sized tendon defect *in vivo,* and MSCs seeded onto the biotextiles promote tendon regeneration and biological integration of the ELAC construct. Given prior reports on their immunomodulatory properties,[33,34] MSCs sourced from allogeneic donor rabbits in this same study were utilized, to avoid the requirement for two major surgeries per animal. Repair outcomes were evaluated in terms of biomechanical, histochemical, and immunohistochemical metrics. The ELAC biotextiles were found to be intact and mechanically competent following 3 months of implantation and biological characteristics of tendon were present in the tissue around and within the scaffolds.

MATERIALS AND METHODS

Chemical sources

Type I collagen was purchased from Collagen Solutions (~6 mg/mL, acid soluble, CS028). Genipin was purchased from Wako Pure Chemical Industries (catalog #078–03021, Richmond, VA). Dulbecco's modified eagle medium (DMEM, Low Glucose with sodium pyruvate, catalog #11885), FBS (MSC qualified, catalog #12662029), and penicillin/streptomycin (10,000 U/mL, catalog #15140–122) were purchased from Gibco of Thermo Fisher Scientific. Isopropyl alcohol (2-propanol, catalog #A416–4), 10% neutral-buffered formalin (NBF, catalog #SF100–4), and 70 μm cell strainers (catalog #22–363-548) were from Fisher Scientific. Peracetic acid (PAA, 32% in dilute acetic acid, catalog #269336) was from Sigma-Aldrich. Antibodies were obtained from LifeSpan BioSciences, BioLegend, Thermo Fisher, or Novus Biologicals as indicated.

Scaffold fabrication

Type I collagen was dialyzed and compacted between two stainless steel wire electrodes (30 V, 90 s) to form ELAC threads as described previously.[27–30] Individual threads were combined to form 3-ply yarns before crosslinking in genipin solution (2% w/v in 90% ethanol) for 72 h at 37°C. Yarns were woven manually around an array of seven stainless steel pins (1.47 mm diameter, 2 mm center-to-center spacing) to a height of 5 mm to form a scaffold unit, which was then embedded in PLGA/chloroform solution (~5% w/v), and slid off of the pins. Two scaffold units were then stacked in parallel and consolidated using a weft fiber passed through the pin-holes to produce a biotextile scaffold (dimensions: ~14 × 5 × 3 mm^3) as shown in Figure 1. PLGA was then removed from the complete scaffolds by immersion in chloroform (2 × 5 min) and scaffolds were air dried to remove residual chloroform. Finally, woven scaffolds were sterilized prior to further use by treating for 4 h in PAA/ethanol solution (1%/22.5% v/v in DI water).

Rabbit mesenchymal stem cell (MSC) isolation and culture

Bone marrow was harvested from femurs of 8 to 11-month-old New Zealand White (NZW) rabbits. Both femurs were rinsed in sterile PBS and the distal epiphyses were rongeured off. The femurs were placed with open, distal end downward in 50 mL centrifuge tubes and spun at 2,000 rpm (600 g) for 1 min to extract bone marrow from the femurs. The bones were then removed from the centrifuge tubes and the remaining bone marrow was diluted in sterile PBS and agitated to release cells. The suspension was then passed through a 70 μm cell strainer to remove clumps. The filtered suspension was centrifuged at 1200 rpm (220*g*) for 5 min to form a cell pellet. Supernatant was poured off and the pellet was resuspended in 10 mL sterile red blood cell lysis buffer (150 m*M* ammonium chloride, 10 m*M* sodium bicarbonate, and 1 m*M* EDTA dissolved in distilled water) for 10 min. The solution was then centrifuged at 1,200 rpm (220*g*) for 5 min, the supernatant was poured off, and the cell pellet was suspended in growth medium (89% DMEM, 10% FBS, 1% penicillin/streptomycin). Cells were seeded on 100 mm tissue culture polystyrene dishes (5 dishes per rabbit harvested), and medium was replaced on day 3 after a rinse with sterile PBS. All cells were given fresh medium every 3 days, were passaged before reaching confluence, and were never frozen. The first passage was typically ~12 days after the initial seeding. Cells were expanded until passage 2, at which point they were detached using Accutase (Innovative Cell Technologies, Inc.) and flow sorted to select for cells that expressed known markers of rabbit MSCs.[35]

Flow sorting of rabbit MSCs

Accutase-detached cells were suspended in FACS buffer at 10^7 cells/mL, and labeled with conjugated antibodies for CD44 (H-CAM Antibody Hermes-1, MA4400; Thermo Fisher Scientific), CD45 (Anti-CD45RB Antibody FITC LS-C43293; LifeSpan BioSciences), and CD90 (Brilliant Violet 421 anti-rat CD90/mouse CD90.1 Thy-1.1, 202529; BioLegend). The unconjugated CD44 antibody was conjugated using DyLight 650 Fast Conjugation Kit (Abcam, catalog #ab201803) according to manufacturer instructions prior to incubation with the cells. Briefly, 1 μL of DyLight Modifier was mixed with 10 μL of CD44 antibody, and these were mixed with Dylight 650 lyophilized conjugation mix. After 15 min in the dark at

room temperature, 1 μL of DyLight Quencher was added. The conjugated CD44 antibody mixture was then used after 5 min. For labeling, 10 μL CD45 antibody, 20 μL CD90 antibody, and 10 μL CD44 antibody were used per 10^7 cells in 1 mL. Cells were incubated with the antibodies at 4°C for 2 h, protected from light. Labeled cells were washed thrice in FACS buffer, then suspended in growth medium at a density of 10^7 cells/mL and flow sorted (BD FACSAria SORP, Becton-Dickinson) to select for cells that were CD44+, CD45−, and CD90−.

Cell seeding of scaffolds

Flow sorted cells were expanded in culture and seeded on scaffolds for surgery at passage 5. Scaffolds were seeded by placing them in custom-made, close-fitting (~17 × 7 × 5 mm), sterile PDMS wells and seeding once daily for three consecutive days with a concentrated suspension of cells in growth medium (5×10^5 cells at 1×10^6 cells/mL on the first and second days, 2.5×10^5 cells at 5×10^5 cells/mL on the third day). Cell attachment was visible on the fibers on the edges of the scaffold (Figure S1). ELAC scaffolds were transferred to the operating room while submerged in 3 mL growth medium within a loosely capped sterile 15 mL centrifuge tube on the day following the third and final seeding.

Animal surgeries

All animal procedures were performed in accordance with established protocols pre-approved by the Institutional Animal Care and Use Committee at the senior author's institution. Sixteen adult female (~8–13 months, 3–5 kg) NZW Rabbits (Charles River Laboratories, Wilmington, MA) underwent surgical creation of a unilateral infraspinatus tendon defect in the right shoulder, while the left shoulder served as an intact control in each specimen (Figure 2a). Infraspinatus tendons were sharply detached at the enthesis, and after burring of the original footprint, were either reattached directly using 3–0 ethibond suture in a Krackow pattern and secured to the humerus using bone tunnels as an operative control (direct repair, $n = 5$, Figure 2b), or a critically sized (≥5 mm), irreparable defect was created and the resulting tendon-bone gap bridged using a woven ELAC scaffold (Figure 2c,d) either by itself (scaffold-alone, $n = 6$) or preseeded with P5 allogeneic marrow-derived CD44+/CD45−/CD90− MSCs (cell-seeded scaffold repair, $n = 5$). The overlapping tendon and scaffold were sutured with 3–0 Ethibond braided suture (Ethicon) using a Krackow pattern in which three locking loop pairs held the tendon,[36] and the tendon/scaffold was re-anchored to the infraspinatus insertion via bone tunnels through the bicipital groove (Figure 2b–d). After surgery, rabbits ambulated freely without weight bearing restrictions and were euthanized at 3 months post-operatively. The time-point of 3 months was selected to provide adequate time for initial recovery of tendon biomechanical properties.[37] Following euthanasia, scapulohumeral complexes were harvested bilaterally, and the infraspinatus muscles were dissected from the rest of the scapula to isolate humerus-tendon-muscle units. Four animals per group were used for biomechanical testing of repair strength. Histology was performed on a single set of non-biomechanically tested specimens from each group, in addition to remnant tissues following biomechanical testing when possible (totals of three animals/group in direct repair and four animals/group in scaffold-alone and cell-seeded scaffold repair).

Biomechanical testing

Biomechanical tests were completed within 18 h of sacrifice, and samples were kept hydrated with PBS until testing was complete. Humeri were potted in aluminum blocks with acrylic cement (Millennium Pour, Keystone Industries). Aluminum blocks were then clamped, the infraspinatus muscle was held in grips cooled with dry ice, and the muscle was pulled perpendicular to the insertion of the original enthesis in monotonic tension at 10 mm/min using a materials testing machine (Test Resources 800LE3-2; Test Resources Inc., MN).[38] For each of the experimental specimens, the intact, contralateral shoulder from the same animal served as the control used for data normalization.

Stiffness and max load values were extracted from load–displacement (L–D) data and normalized to intact contralateral values and location of the failure was noted (attachment vs. mid-substance). Linear regression was performed on elastic regions of L–D curves from 40% to 60% of the max load value, and slope of the best-fit line was taken to be stiffness (R^2 values were ≥0.95).

Histology and immunohistochemistry

Harvested specimens were fixed in 10% NBF prior to decalcification using Immunocal (Statlab Medical Products, McKinney, TX). Decalcified specimens were processed, embedded in paraffin, and slides with 5 μm sections were obtained in planes as illustrated in Figure S2 which highlights the cortical bone, tendon, muscle, scaffold, and tissue response around the scaffold. Slides were then stained with Masson's Trichrome for collagen deposition and Hematoxylin & Eosin (H&E) for general morphology. Histology and immunohistochemistry (IHC) was also performed for collagen I (Collagen I alpha 1 Antibody, catalog #NB600–450; Novus Biologicals), collagen III (Collagen III alpha 1 Antibody, catalog #NBP1–05119, Novus Biologicals), procollagen I (SP1.D8; Iowa Developmental Studies Hybridoma Bank), and tenomodulin (Tenomodulin Antibody aa74–123, HRP conjugated, catalog #LS-C452705; LifeSpan BioSciences). A conjugated secondary antibody (Goat anti-Mouse IgG HRP, catalog #HAF007; Novus Biologicals) was utilized with the unconjugated primary antibodies (collagen I, collagen III, and procollagen I). Slides were imaged with a bright-field microscope (Olympus IX83; Olympus Corp., Tokyo, Japan), and assessed for collagen deposition (Masson's trichrome) and cellularity (H&E).

Stained slides were examined and semi-quantitatively scored by a senior pathologist (J. Anderson) in accordance with modified ISO 10993-6 and ASTM F981-04 standards.[39,40]. Metrics associated with tendon tissue, namely, collagen fiber structure and alignment, rounding of nuclei, cell population, and chronic inflammation were each scored from 0 to 3 (Table I), based on qualifications from methods in the literature, where a score of zero (0) in each category represents native tendon.[8,39–44]

In addition to semi-quantitative scoring, the total number of cell nuclei present within a high-powered field (HPF) (400× magnification) was assessed quantitatively in sections stained with H&E. For cell counts, images under the high-powered field from five non-overlapping regions within and five non-overlapping regions outside the continuum of the

ELAC scaffold were collected from three slides of four specimens from within scaffold-alone and cell-seeded groups for a total of 12 slides analyzed per group.

Histology and immunohistochemistry-stained specimens were assessed in a binary fashion for staining of collagen I, collagen III, tenomodulin, and procollagen I ($n = 3$ for treatment groups, $n = 2$ for native tendon) and the number of positive specimens recorded (Table II). Scaffold alone and cell-seeded scaffold groups were further split into two categories: "inside," referring to regions within the continuum of the scaffold and "outside," denoting regions in the tissue surrounding the scaffold material.

Computerized image analysis for collagen deposition

Scans of Masson's trichrome-stained specimens were analyzed via a custom MATLAB program to determine the percentage of *de novo* collagen in the tissue area within the scaffolds for both scaffold-alone and cell-seeded scaffold repairs. Prior to analysis, the scaffold region was manually isolated using ImageJ and the total area was recorded. In MATLAB, the Red-Green-Blue (RGB) image of the scaffold region underwent two masking steps. The first masking step isolated the void spaces in order to remove this area from the percentage calculations by thresholding channels 1, 2, and 3 as 209:255, 208:255, and 212:255, respectively. Void spaces are an artifact of the sectioning process. The second masking step isolated the *de novo* collagen as indicated by the blue area of the Masson's trichrome images by thresholding channels 1, 2, and 3 as 19.27:100.00, 22.032:64.45, and −75.48: −9.00, respectively. This thresholding was chosen manually using MATLAB's Color Thresholder and used for analysis of all specimens. The percentage of the scaffold area attributable to *de novo* collagen formation was then calculated as:

$$P_{dn} = A_{dn}/(A_t - A_v)$$

Where A_{dn} is the calculated area of the *de novo* collagen production, A_t is the total scaffold area, and A_v is the area attributable to voids.

Statistical analysis

Stiffness and max load data were assessed for significant differences using the Kruskal–Wallis test (significance set at $p \leq 0.05$); where significance was indicated, pairwise comparisons were performed among treatment groups using Mann–Whitney *U*-test (significance set at $p \leq 0.05$). Quantitative histological measurements were also analyzed using the Mann–Whitney *U*-test (significance set at $p \leq 0.05$).

RESULTS

Surgical post-op and harvest

No peri-operative or post-operative complications were encountered. All rabbits survived to the end of the survival period, and rabbits in all three groups recovered and were observed to ambulate and bear weight beginning on post-operative days 2 or 3. One rabbit from the cell-seeded scaffold group pulled out its skin sutures, resulting in self-inflicted wound dehiscence during the course of post-operative recovery, and heterotopic bone formation was

noted during the harvest of this specimen after 3 months *in vivo.* All woven scaffold specimens were found to be intact and firmly anchored to the humeral head at the time of harvest.

Biomechanical testing

The group repaired with cell-seeded scaffolds demonstrated a statistically significant increase in stiffness relative to the scaffold-alone group (Figure 3a). However, no significant difference in max load was observed (Figure 3b). No significant differences were found between the scaffold-alone and direct repair, or direct repair and cell-seeded scaffold groups.

Intact and direct-repair specimens failed consistently at the interface between the soft tissue and bone. Conversely, cell-seeded scaffold repairs failed consistently within the midsubstance. Scaffold-alone repairs displayed a mixed mode failure where three of the specimens failed at the interface while the remaining two failed at the midsubstance (Figure 4). As shown, 13 shoulder pairs were assessed for failure location. However, one pair has been excluded from calculations of stiffness and max load due to slipping of the control shoulder during mechanical testing.

Histology and immunohistochemistry

Histological scoring (Table I) demonstrated collagen fiber structure and arrangement consistent with tendon tissue. Signs of chronic inflammation were absent in direct repair and cell-seeded groups. Minimal indications of chronic inflammation were present in the scaffold-alone group. Masson's Trichrome staining indicated collagen deposition both within the continuum of the scaffold and the surrounding tissue in all groups (Figures 5–7).

For semi-quantitative scoring, higher populations of nucleated cells were noted in scaffold-alone (1.95 ± 0.17) and cell-seeded (2.25 ± 0.24) groups compared to direct repair (1.33 ± 0.38) (Table I). Quantitative assessment of cellularity confirmed a significantly greater ($p < 0.001$) quantity of nucleated cells was present within the continuum of the scaffolds in the cell-seeded group as compared to the scaffold-alone group. Additionally, there was a statistically significant ($p < 0.001$) increase in the number of nucleated cells within the continuum of the scaffold when compared to the encapsulating tissue for both treatment groups (Figure 8).

Histology and immunohistochemistry results confirmed the presence of collagen I, collagen III, procollagen I, and tenomodulin within and immediately outside of the continuum of the scaffolds in both the ELAC scaffold-alone and MSC-seeded groups (Figure 9). The direct repair group was also positive for collagen I, collagen III, but tenomodulin and procollagen I staining was notably absent in the direct repair specimens.

Computerized image analysis for collagen deposition

Cell-deposited collagen followed the contour of ELAC threads in both groups (Figures 6 and 7). Computerized analysis of Masson's trichrome stained samples for *de novo* collagen deposition found no significant difference in area fraction of cell-deposited collagen between

scaffold-alone and cell-seeded scaffold repairs as determined by Mann-Whitney analysis ($p = 0.34$).

DISCUSSION

While many current approaches augmenting rotator cuff tendon healing focus on utilization of synthetic or natural materials to augment and accelerate repair,[11] several setbacks using these approaches have been identified. Material composition is a major concern, as synthetic materials capable of possessing appropriate mechanical properties are easy to produce[12,14,41] however these materials often fail to provide the biological cues necessary to stimulate and guide tissue integration. In contrast, biologically sourced, decellularized matrices contain biological molecules appropriate for tissue integration, however remnant cellular components (small proteins, cell fragments, DNA/RNA fragments, etc.) may remain within the matrix following the decellularization process that could provoke detrimental biological responses (i.e., inflammation).[45] In addition, while decellularized matrices are eventually remodeled, cellular migration into the matrix is often limited by its physical structure (i.e., densely packed extracellular matrix in native tendon) that necessitates further modification to facilitate ease of cell infiltration.[10,46] Lastly, manipulation of decellularized ECM mechanical properties to match the native tissue in need of repair may be difficult in cases where the starting ECM is derived from a non-tendon source.

The approach to augmenting critically sized, irreparable tendon defects[47] detailed in this work was designed to address many of these key limitations encountered in current rotator cuff tendon repair methods. A purified solution of the primary protein component of tendon ECM, collagen type I, was electrochemically aligned and compacted into thin fibers that were woven into scaffolds. These woven scaffolds have demonstrated robust mechanical properties similar to that of native tendon, ample porosity for cellular infiltration and integration, along with biological cues to induce appropriate cellular responses (cell attachment and tissue integration, resorption, and remodeling).[27–29] Prior mechanical tests of ELAC threads have shown an ultimate stress of 65 MPa while scaffolds woven from ELAC threads demonstrated a Young’s modulus of 500 MPa, and similar to the native infraspinatus tendon in rabbits, with both the native tendon and ELAC displaying an initial toe region where the material was initially compliant before stiffening with increasing displacement.[28] Most importantly, the woven structure was robust to the extent that it held sutures and it was implantable in a fully load-bearing context. While these previous experiments assessed functional advantages to tissue repair *in vitro,* results from this investigation demonstrated the benefits to rotator cuff tendon repair *in vivo* in a full load-bearing capacity.

The max load and stiffness of scaffold-alone and direct repairs were comparable, demonstrating that ELAC scaffold repairs match the strength of the clinical standard (suture-based, direct repair). Biomechanical testing data suggest that addition of MSCs to woven collagen scaffolds may enhance repair stiffness and strength. Furthermore, MSC supplementation likely enhanced the integration between the bone and the scaffold as reflected by consistent failure occurring at the midsubstance region. This is potentially the result of cell-mediated integration between soft (tendon) and hard (bone) tissues.

It should be noted that one specimen in the cell-seeded group exhibited significant heterotopic over-growth around the scaffold in the region of the humeral head that was decorticated during the course of surgery, as the irritation typically associated with growth of heterotopic bone[48] was the likely reason the rabbit removed its skin sutures with continued irritation at the incision site over the course of 6 weeks following the surgery. It should also be noted that heterotopic ossification is a well-documented phenomenon in cases of total joint arthroplasty in humans, occurring in up to 15% of patients undergoing total shoulder replacement.[49] Reported rates are as high as 36% when concomitant rotator cuff arthropathy is present,[49] as well as in cases of open rotator cuff repair, in which occurrence rates are present in 26% of patients.[50]

Histological staining with Masson's trichrome revealed the presence of *de novo* collagen between ELAC fibers for both scaffold-alone and cell-seeded scaffold repairs, while collagen appeared to follow the contour of ELAC threads. This suggests that ELAC serves as a template for guiding cellular collagen deposition. Collagen fiber alignment and arrangement were of particular interest in the tissue surrounding the scaffolds in the two treatment groups as the tissue exhibited overall structure that was similar to native tendon tissue as reflected by total histological scores (Figures 6–8 and Table I). It should be noted that biomechanically tested remnant tendon/muscle specimens did exhibit minor artifact as a result of testing and regions where tissue was clearly disrupted (sizeable gaps, frayed tissue edges, etc.) were omitted from our tendon scoring assessment.

As demonstrated by H&E staining, both groups exhibited increased cell density within the ELAC scaffold as compared to the tissue encapsulating the scaffold material (Figure 8). Additionally, specimens within the cell-seeded scaffold repair group exhibited higher cell density within the continuum of the scaffold in comparison to the scaffold-alone group. The cells present in the scaffolds originally seeded with MSCs could be of two potential origins. They could be the originally seeded MSCs and/or they could be host cells drawn to the area as a result of paracrine effects. The presence of collagen in scaffold only group implies that host cells are capable of infiltrating and synthesizing de-novo collagen. It is possible that cell-seeded group may have benefited from collagen production from both host and allogeneic cells. However, the experimental design of this investigation did not allow for distinguishing between the two cell sources. To address this limitation, future studies could consider implantation of stem cells that stably express a label or distinguishing marker.[51]

The IHC results of primary significance were for the tendon-specific marker, tenomodulin. Both within the interior and immediately outside of the scaffold, tenomodulin was present in scaffold-alone and cell-seeded scaffold groups. This suggests that not only do the cells infiltrating and surrounding the ELAC fibers produce the primary ECM protein associated with tendon (collagen I) and exhibit visible characteristics similar to native tendon (aligned ECM, elongated shape, low vascularity, etc.), they also express a tendon-specific marker. These data are in agreement with previous experiments *in vitro* which demonstrated there is upregulation of scleraxis and increased tenomodulin production in MSCs seeded onto ELAC threads.[28,30] A notable finding from these experiments *in vivo* is that the ELAC fibers within the group containing the scaffold alone (no MSCs) appear to be sufficient to induce tenogenic differentiation of the cells that infiltrate and encapsulate the scaffold, as no

significant differences in presence of tenomodulin were noted between scaffold-alone and cell-seeded groups (Figure 9 and Table II).

As noted previously, the direct repair mimics the best-case operative scenario in that the tendon was immediately reattached following initial detachment. Clinically, this group emulates ideal rotator cuff repair conditions where there is no significant degeneration of the original tendon prior to the repair (i.e., acute injury). Despite immediate reattachment, a regression in the tendon phenotype of direct repair was observed such that the tendon-specific marker tenomodulin was largely absent in the remnant tendon (Figure 9 and Table II). Similarly, collagen matrix production by resident cells as reflected by procollagen I was notably absent in the tendon remnants of the direct repair group in comparison to treatment groups. Cumulatively, these observations suggest that the inherent regenerative capacity of tendon is limited even in ideal conditions.

The presence of *de novo* collagen within the scaffolds warranted further characterization by IHC staining to identify the collagen types present. IHC results confirm that scaffolds composed of ELAC threads likely promote deposition of collagens type I and type III, both within the continuum of the scaffolds as well as within the immediate, surrounding tissue (Figure 9). Qualitatively, collagen type I appeared in greater abundance overall in comparison to collagen type III. Additionally, procollagen I was found within cells throughout the continuum of the ELAC scaffold and highlights continued matrix synthesis after 3 months of implantation.

A limitation of this investigation is the sample size of each group was low; as such, many findings presented may be phenomenological. Another limitation is that the repairs performed in this study mimicked a best-case scenario in that the ruptured rotator cuff tendon underwent immediate repair. In the direct repair group, the tendon was detached and reattached in the same surgical procedure whereas many rotator cuff tendon failures do not undergo immediate repair and are subject to tissue degeneration and fatty tissue infiltration if untreated for significant periods of time. It should also be noted that significant artifacts were observed upon histological examination of the biomechanically tested specimens that complicated analysis of collagen fiber structure and arrangement. However, this study presents a novel approach which may hold merit for the repair and regeneration of critically-sized tendon defects.

In conclusion, this study demonstrates key benefits of utilizing woven collagen biotextiles for the repair of critically-sized tendon defects. Woven ELAC scaffolds possess sufficient mechanical strength for surgical manipulation, can be sterilized and stored in advance of surgery, and remain intact after 3 months in a fully load-bearing capacity *in vivo.* Biomechanical testing highlighted possible synergistic effects of combining MSCs and ELAC threads with respect to increasing stiffness of the repair. Histological findings are notable in that the tissue regenerated within and around the scaffolds was composed primarily of collagen type I and a key tendon protein, tenomodulin, present within the scaffold-alone and cell-seeded scaffold groups. Future work will concentrate on elucidating the effects of woven collagen biotextiles in rotator cuff tendon repairs using a larger number of specimens per group and over a longer post-operative period (6 months).

Supplementary Material

Refer to Web version on PubMed Central for supplementary material.

ACKNOWLEDGMENTS

This study was supported by grants from National Institutes of Health (NIH): R01 AR063701 (OA) and T32 AR007505 (GL and VW). The authors are grateful for core facility services and expertise provided by the Animal Resource Center and the Cytometry & Imaging Microscopy Shared Resource (P30CA043703) at CWRU. Additionally, the corresponding author (OA) holds primary ownership of Collgen LLC.

Contract grant sponsor: National Institutes of Health; contract grant number: T32 AR007505, R01 AR063701

REFERENCES

1. Galatz LM, Ball CM, Teefey SA, Middleton WD, Yamaguchi K. The outcome and repair integrity of completely arthroscopically repaired large and massive rotator cuff tears. J Bone Joint Surg Am 2004;86:219–224. [PubMed: 14960664]
2. Mather RC, Koenig L, Acevedo D, Dall TM, Gallo P, Romeo A, Tongue J, Williams G. The societal and economic value of rotator cuff repair. J Bone Joint Surg Am 2013;95:1993–2000. [PubMed: 24257656]
3. McElvany MD, McGoldrick E, Gee AO, Neradilek MB, Matsen FA. Rotator cuff repair: Published evidence on factors associated with repair integrity and clinical outcome. Am J Sports Med 2015;43: 491–500. [PubMed: 24753240]
4. Gladstone JN, Bishop JY, Lo IKY, Flatow EL. Fatty infiltration and atrophy of the rotator cuff do not improve after rotator cuff repair and correlate with poor functional outcome. Am J Sports Med 2007;35:719–728. [PubMed: 17337727]
5. Miyazaki AN, Santos PD, da Silva LA, Sella G do V, Miranda ER de AB, Zampieri R. Fatty muscle infiltration in cuff tear: Pre and post operative evaluation by MRI. Acta Ortopedica Bras 2015;23: 251–254.
6. Rubino LJ, Sprott DC, Stills HF, Crosby LA. Fatty infiltration does not progress after rotator cuff repair in a rabbit model. Art Ther 2008;24:936–940.
7. Randelli P, Cucchi D, Ragone V, de Girolamo L, Cabitza P, Randelli M. History of rotator cuff surgery. Knee Surg Sports Traumatol Arthrosc 2015;23:344–362. [PubMed: 25448135]
8. Chen JM, Willers C, Xu J, Wang A, Zheng M-H. Autologous tenocyte therapy using porcine-derived bioscaffolds for massive rotator cuff defect in rabbits. Tissue Eng 2007;13:1479–1491. [PubMed: 17536925]
9. Derwin KA, Badylak SF, Steinmann SP, lannotti JP. Extracellular matrix scaffold devices for rotator cuff repair. J Shoulder Elbow Surg 2010;19:467–476. [PubMed: 20189415]
10. Pan J, Liu G-M, Ning L-J, Zhang Y, Luo J-C, Huang F-G, Qin T-W. Rotator cuff repair using a decellularized tendon slices graft: An in vivo study in a rabbit model. Knee Surg Sports Traumatol Arthrosc 2015;23:1524–1535. [PubMed: 24623185]
11. Gillespie RJ, Knapik DM, Akkus O. Biologic and synthetic grafts in the reconstruction of large to massive rotator cufftears. J Am Acad Orthop Surg 2016;24:823–828. [PubMed: 27768610]
12. Inui A, Kokubu T, Mifune Y, Sakata R, Nishimoto H, Nishida K, Akisue T, Kuroda R, Satake M, Kaneko H, Fujioka H. Regeneration of rotator cuff tear using electrospun poly(d,l-lactide-co-glycolide) scaffolds in a rabbit model. Arthrosc J Arthrosc Relat Surg 2012;28: 1790–1799.
13. Inui A, Kokubu T, Fujioka H, Nagura I, Sakata R, Nishimoto H, Kotera M, Nishino T, Kurosaka M. Application of layered poly (l-lactic acid) cell free scaffold in a rabbit rotator cuff defect model. Sports Med Arthrosc Rehabil Ther Technol 2011;3:29. [PubMed: 22136125]
14. Yokoya S, Mochizuki Y, Nagata Y, Deie M, Ochi M. Tendon-bone insertion repair and regeneration using polyglycolic acid sheet in the rabbit rotator cuff injury model. Am J Sports Med 2008;36: 1298–1309. [PubMed: 18354143]

15. Kim Y-S, Lee H-J, Ok J-H, Park J-S, Kim D-W. Survivorship of implanted bone marrow-derived mesenchymal stem cells in acute rotator cuff tear. J Shoulder Elbow Surg 2013;22:1037–1045. [PubMed: 23246275]
16. Gulotta LV, Rodeo SA. Growth factors for rotator cuff repair. Clin Sports Med 2009;28:13–23. [PubMed: 19064162]
17. Gulotta LV, Kovacevic D, Montgomery S, Ehteshami JR, Packer JD, Rodeo SA. Stem cells genetically modified with the developmental gene MT1-MMP improve regeneration of the supraspinatus tendon-to-bone insertion site. Am J Sports Med 2010;38:1429–1437. [PubMed: 20400753]
18. Gulotta LV, Kovacevic D, Packer JD, Deng XH, Rodeo SA. Bone marrow-derived mesenchymal stem cells transduced with scleraxis improve rotator cuff healing in a rat model. Am J Sports Med 2011; 39:1282–1289. [PubMed: 21335341]
19. Gulotta LV, Kovacevic D, Packer JD, Ehteshami JR, Rodeo SA. Adenoviral-mediated gene transfer of human bone morphogenetic protein-13 does not improve rotator cuff healing in a rat model. Am J Sports Med 2011;39:180–187. [PubMed: 20956264]
20. Pelinkovic D, Lee J-Y, Engelhardt M, Rodosky M, Cummins J, Fu F, Huard J. Muscle cell-mediated gene delivery to the rotator cuff. Tissue Eng 2003;9:143–151. [PubMed: 12625963]
21. Testa S, Costantini M, Fornetti E, Bernardini S, Trombetta M, Seliktar D, Cannata S, Rainer A, Gargioli C. Combination of biochemical and mechanical cues for tendon tissue engineering. J Cell Mol Med 2017;21:2711–2719. [PubMed: 28470843]
22. Wu S, Wang Y, Streubel PN, Duan B. Living nanofiber yarn-based woven biotextiles for tendon tissue engineering using cell triculture and mechanical stimulation. Acta Biomater 2017;62: 102–115. [PubMed: 28864251]
23. Butler DL, Juncosa-Melvin N, Boivin GP, Galloway MT, Shearn JT, Gooch C, Awad H. Functional tissue engineering for tendon repair: A multidisciplinary strategy using mesenchymal stem cells, bioscaffolds, and mechanical stimulation. J Orthop Res 2008;26:1–9. [PubMed: 17676628]
24. Juncosa-Melvin N, Boivin GP, Galloway MT, Gooch C, West JR, Sklenka AM, Butler DL. Effects of cell-to-collagen ratio in mesenchymal stem cell-seeded implants on tendon repair biomechanics and histology. Tissue Eng 2005;11:448–457. [PubMed: 15869423]
25. Juncosa-Melvin N, Boivin GP, Gooch C, Galloway MT, West JR, Dunn MG, Butler DL. The effect of autologous mesenchymal stem cells on the biomechanics and histology of gel-collagen sponge constructs used for rabbit patellar tendon repair. Tissue Eng 2006; 12:369–379. [PubMed: 16548695]
26. Cheng X, Gurkan UA, Dehen CJ, Tate MP, Hillhouse HW, Simpson GJ, Akkus O. An electrochemical fabrication process for the assembly of anisotropically oriented collagen bundles. Biomaterials 2008;29:3278–3288. [PubMed: 18472155]
27. Kishore V, Uquillas JA, Dubikovsky A, Alshehabat MA, Snyder PW, Breur GJ, Akkus O. In vivo response to electrochemically aligned collagen bioscaffolds. J Biomed Mater Res B Appl Biomater 2012; 100B:400–408.
28. Younesi M, Islam A, Kishore V, Anderson JM, Akkus O. Tenogenic induction of human MSCs by anisotropically aligned collagen biotextiles. Adv Funct Mater 2014;24:5762–5770. [PubMed: 25750610]
29. Uquillas JA, Kishore V, Akkus O. Effects of phosphate-buffered saline concentration and incubation time on the mechanical and structural properties of electrochemically aligned collagen threads. Biomed Mater 2011;6:035008. [PubMed: 21540522]
30. Kishore V, Bullock W, Sun X, Van Dyke WS, Akkus O. Tenogenic differentiation of human MSCs induced by the topography of electrochemically aligned collagen threads. Biomaterials 2012;33: 2137–2144. [PubMed: 22177622]
31. Awad HA, Butler DL, Boivin GP, Smith FNL, Malaviya P, Huibregtse B, Caplan A. Autologous mesenchymal stem cell-mediated repair of tendon. Tissue Eng 1999;5:267–277. [PubMed: 10434073]
32. Yin Z, Guo J, Wu T-Y, Chen X, Xu L-L, Lin S-E, Sun Y-X, Chan K-M, Ouyang H, Li G. Stepwise differentiation of mesenchymal stem cells augments tendon-like tissue formation and defect repair in vivo. Stem Cells Transl Med 2016;5:1106–1116. [PubMed: 27280798]

33. Gao F, Chiu SM, Motan DAL, Zhang Z, Chen L, Ji H-L, Tse H-F, Lu Q-L, Lian Q. Mesenchymal stem cells and immunomodulation: Current status and future prospects. Cell Death Dis 2016;7:e2062. [PubMed: 26794657]
34. Caplan AI. Mesenchymal stem cells: Time to change the name! Stem Cells Transl Med 2017;6:1445–1451. [PubMed: 28452204]
35. Lee T-C, Lee T-H, Huang Y-H, Chang N-K, Lin Y-J, Chien P-WC, Yang W-H, Lin MH-C. Comparison of surface markers between human and rabbit mesenchymal stem cells. PLoS ONE 2014;9: e111390. [PubMed: 25380245]
36. Krackow KA, Thomas SC, Jones LC. A new stitch for ligament-tendon fixation. Brief note. J Bone Joint Surg Am 1986;68:764–766. [PubMed: 3522596]
37. Blickenstaff KR, Grana WA, Egle D. Analysis of a semitendinosus autograft in a rabbit model. Am J Sports Med 1997;25:554–559. [PubMed: 9240991]
38. Islam A, Bohl MS, Tsai AG, Younesi M, Gillespie R, Akkus O. Biomechanical evaluation of a novel suturing scheme for grafting load-bearing collagen scaffolds for rotator cuff repair. Clin Biomech Bristol Avon 2015;30:669–675.
39. ISO 10993-6:2016 Biological evaluation of medical devices — Part 6: Tests for local effects after implantation [Internet] [cited November 2, 2017]. https://www.iso.org/standard/61089.html.
40. ASTM F981-04. Standard Practice for Assessment of Compatibility of Biomaterials for Surgical Implants with Respect to Effect of Materials on Muscle and Insertion into Bone. West Conshohocken, PA: ASTM International; 2016.
41. Astrom M, Rausing A. Chronic Achilles Tendinopathy: a survey of surgical and histopathologic findings mats. Clin Orthop 1995;316: 151–164.
42. Shen W, Chen J, Yin Z, Chen X, Liu H, Heng BC, Chen W, Ouyang H-W. Allogenous tendon stem/progenitor cells in silk scaffold for functional shoulder repair. Cell Transplant 2012;21:943–958. [PubMed: 22405331]
43. Zheng Z, Ran J, Chen W, Hu Y, Zhu T, Chen X, Yin Z, Heng BC, Feng G, Le H, Tang C, Huang J, Chen Y, Zhou Y, Dominique P, Shen W, Ouyang H. Alignment of collagen fiber in knitted silk scaffold for functional massive rotator cuff repair. Acta Biomater 2017; 51:317–329. [PubMed: 28093363]
44. Yin Z, Chen X, Song H, Hu J, Tang Q, Zhu T, Shen W, Chen J, Liu H, Heng BC, Ouyang H-W. Electrospun scaffolds for multiple tissues regeneration in vivo through topography dependent induction of lineage specific differentiation. Biomaterials 2015;44:173–185. [PubMed: 25617136]
45. Malcarney HL, Bonar F, Murrell GAC. Early inflammatory reaction after rotator cuff repair with a porcine small intestine submucosal implant: A report of 4 cases. Am J Sports Med 2005;33:907–911. [PubMed: 15827358]
46. Pridgen BC, Woon CYL, Kim M, Thorfinn J, Lindsey D, Pham H, Chang J. Flexor tendon tissue engineering: Acellularization of human flexor tendons with preservation of biomechanical properties and biocompatibility. Tissue Eng PartC Methods 2011;17:819–828.
47. Pietschmann MF, Frankewycz B, Schmitz P, Docheva D, Sievers B, Jansson V, Schieker M, MQller PE. Comparison of tenocytes and mesenchymal stem cells seeded on biodegradable scaffolds in a full-size tendon defect model. J Mater Sci Mater Med 2013;24: 211–220. [PubMed: 23090834]
48. Hinck SMMR. Heterotopic ossification: A review of symptoms and treatment. Rehabil Nurs 1994;19:169–173. [PubMed: 8202622]
49. Boehm TD, Wallace WA, Neumann L. Heterotopic ossification after primary shoulder arthroplasty. J Shoulder Elbow Surg 2005; 14:6–10. [PubMed: 15723007]
50. Erggelet C, Eggensperger G, Steinwachs M, Lahm A, Reichelt A. Postoperative ossifications of the shoulder. Arch Orthop Trauma Surg 1999;119:168–170. [PubMed: 10392512]
51. Abd-Allah SH, Shalaby SM, Pasha HF, El-Shal AS, Raafat N, Shabrawy SM, Awad HA, Amer MG, Gharib MA, El Gendy EA, Raslan AA, El-Kelawy HM. Mechanistic action of mesenchymal stem cell injection in the treatment of chemically induced ovarian failure in rabbits. Cytotherapy 2013;15:64–75. [PubMed: 23260087]

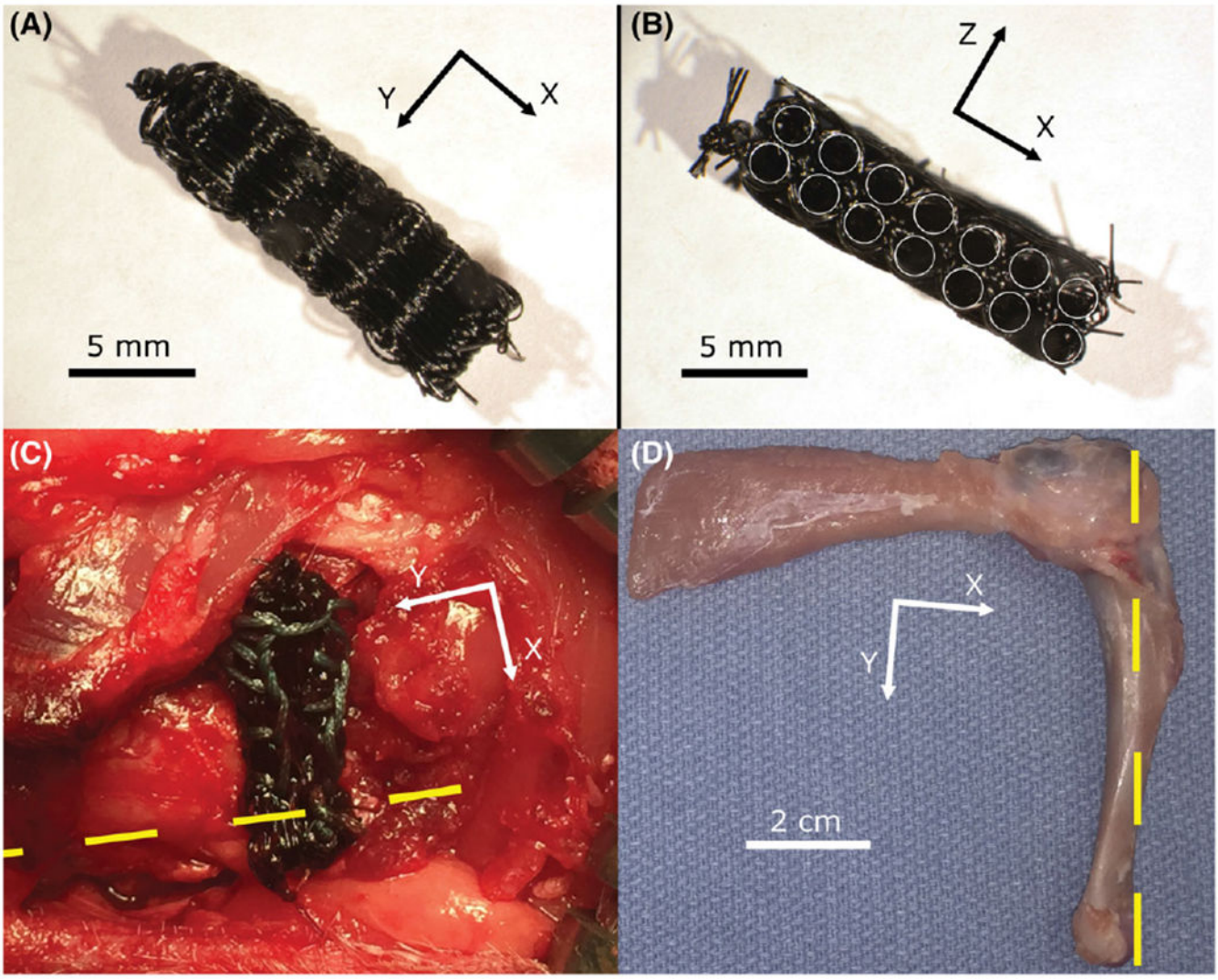

FIGURE 1.

Scaffolds of electrochemically aligned collagen yarns were woven, stacked, and consolidated using a weft fiber to form a complete scaffold (A and B, circular holes highlighted in B). The complete, sterilized scaffold was inserted into a defect created within the right infraspinatus tendon of a rabbit and secured in place on the remaining tendon using 3–0 braided Ethibond suture in a Krackow pattern. The yellow dashed line highlights the longitudinal axis of the diaphysis (C). The humerus, scaffold, and infraspinatus tendon were harvested following 3 months of implantation (D).

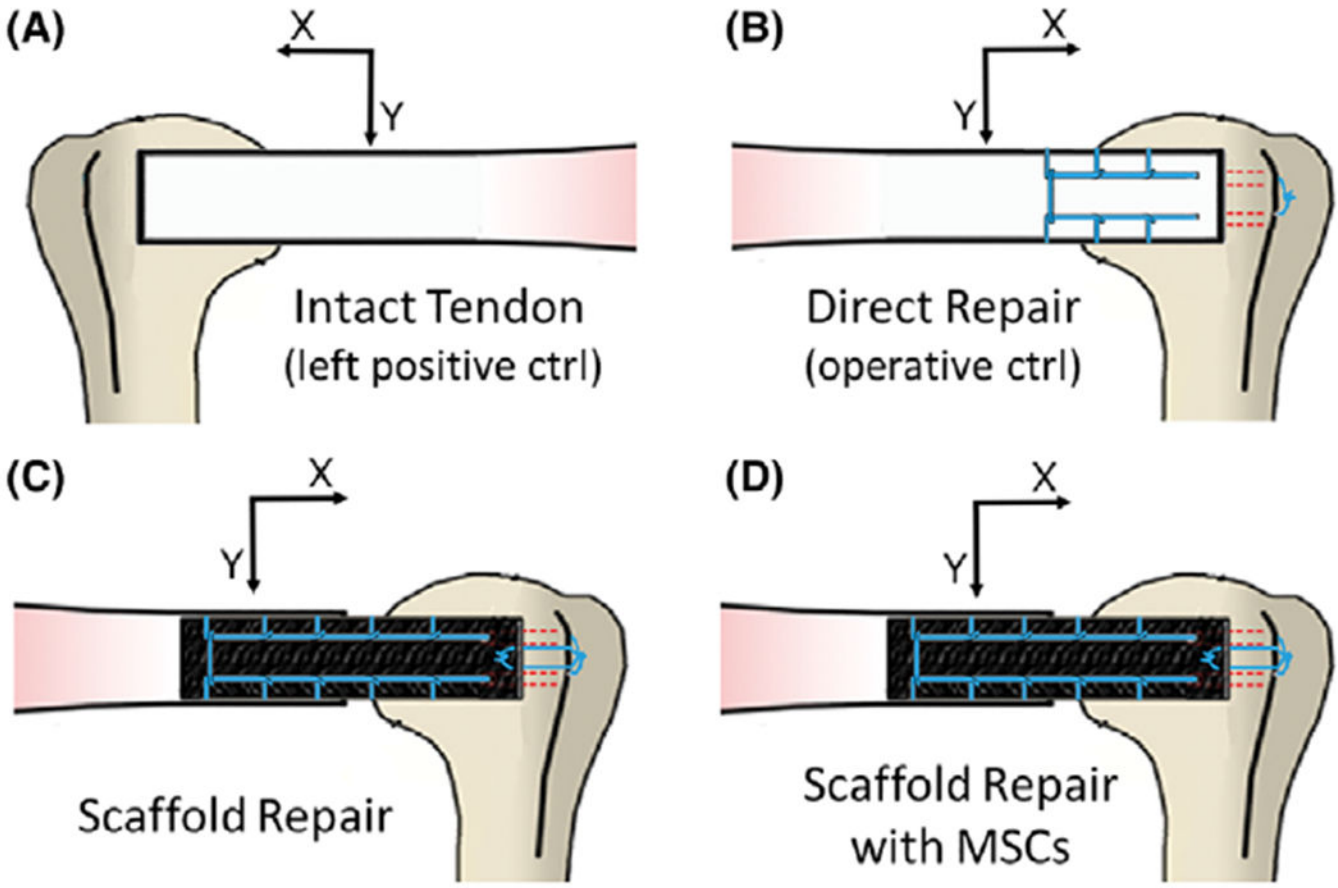

FIGURE 2.

The experimental groups consisted of the intact (left shoulder) infraspinatus tendon in each rabbit (A), a direct repair group where the tendon was sharply detached at the enthesis and immediately reattached (B), a scaffold alone group in which a large defect was introduced in the infraspinatus tendon and the ELAC scaffold was used to bridge the defect (C), and a group of scaffolds seeded with MSCs bridging the defect in the same fashion as the non-cell-seeded group (D).

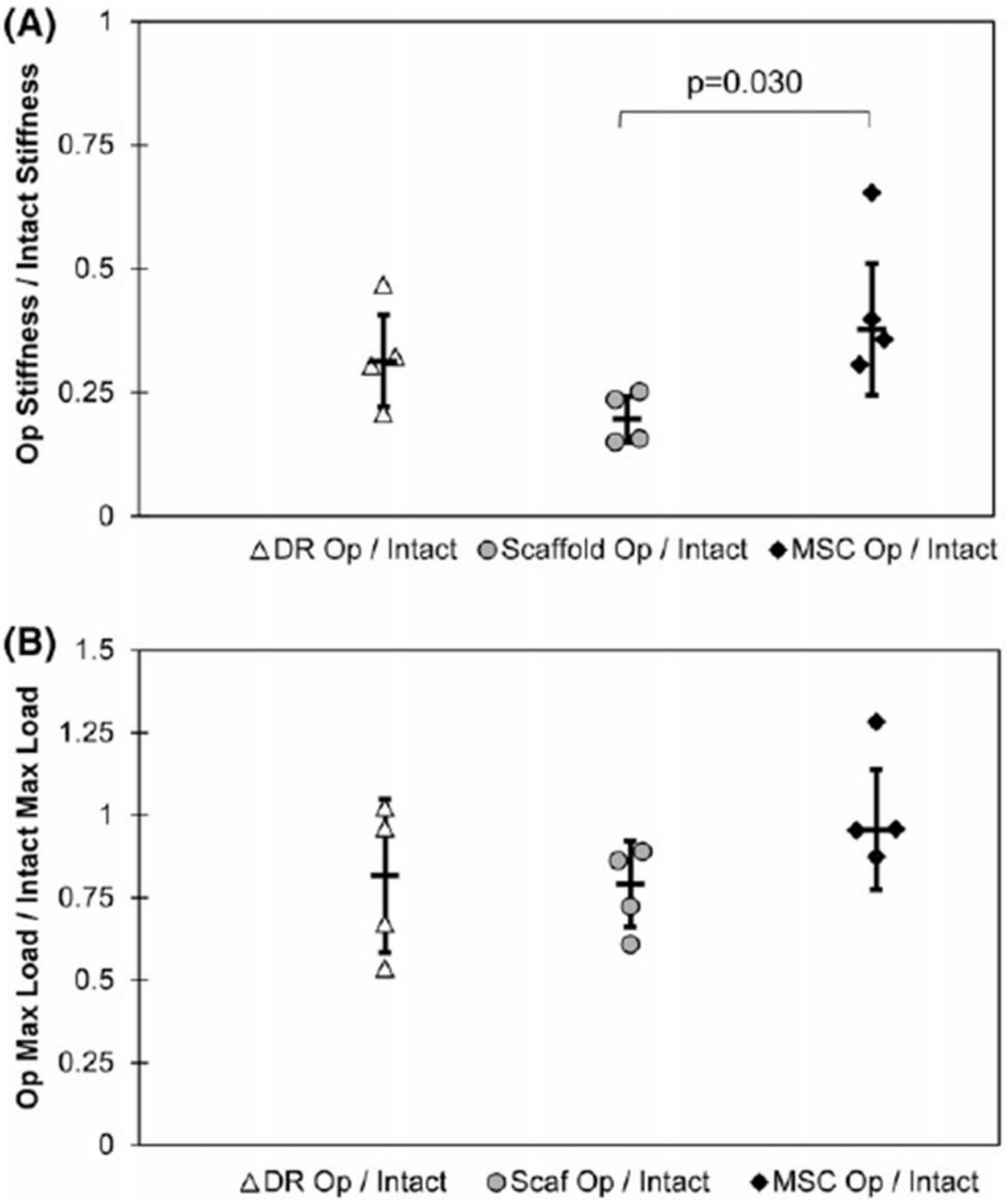

FIGURE 3.

Graphs illustrating biomechanical properties for specimens harvested following 3 months of implantation *in vivo.* A significant difference in stiffness normalized to contralateral intact specimens was noted between the scaffold-alone (Scaf Op/Intact) and cell-seeded scaffold (MSC Op/Intact) groups (A). Comparable results for max load, normalized to intact controls, were observed among all three groups (B). Error bars indicate standard deviation in each graph.

Group / Failure Site	Intact	Direct Repair	Scaffold-alone	Cell-seeded
Interface	13	4	3	0
Midsubstance	0	0	2	4

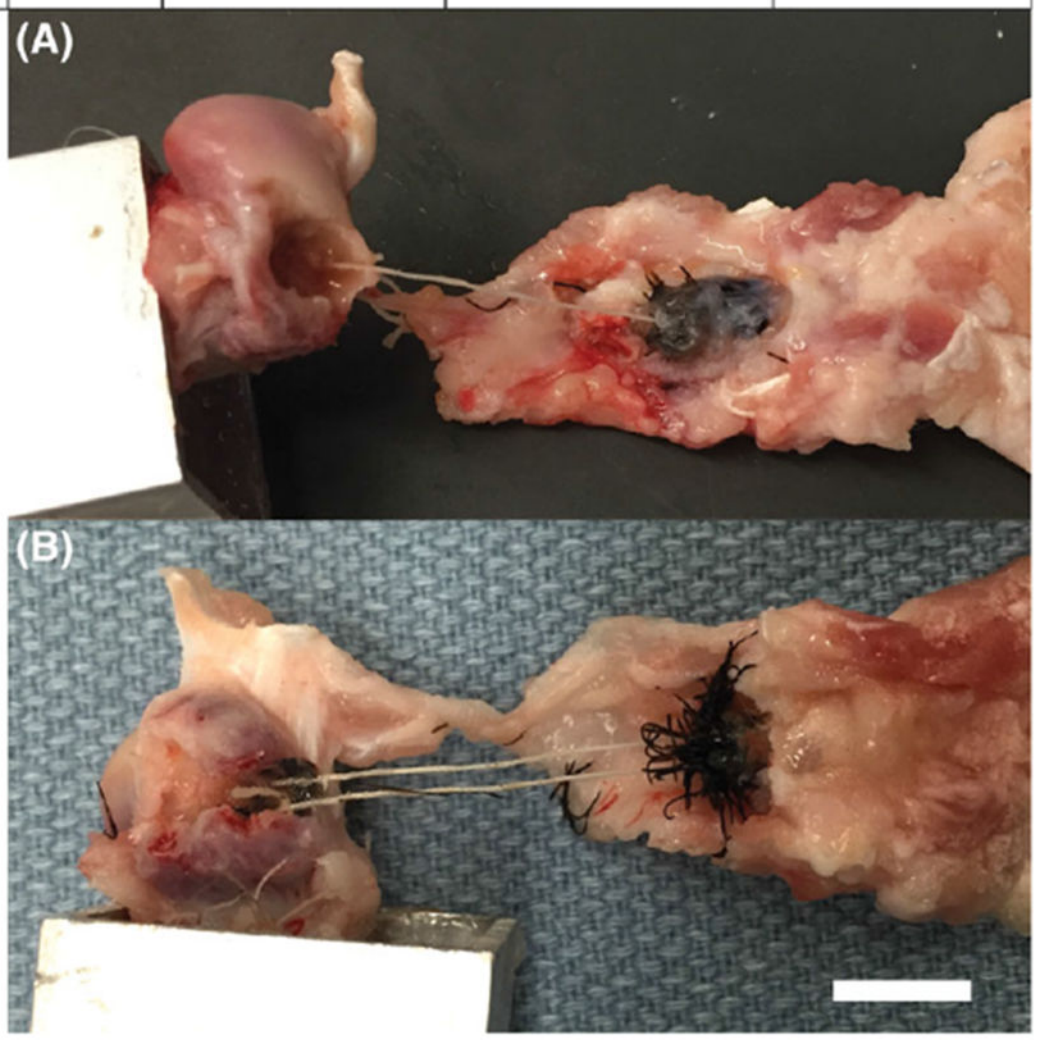

FIGURE 4.
Location of failure during mechanical testing. Failures occurred in two locations, at the interface between the bone and tendon/scaffold (A) and in the midsubstance of the tendon/scaffold (B). Scale bar = 1 cm.

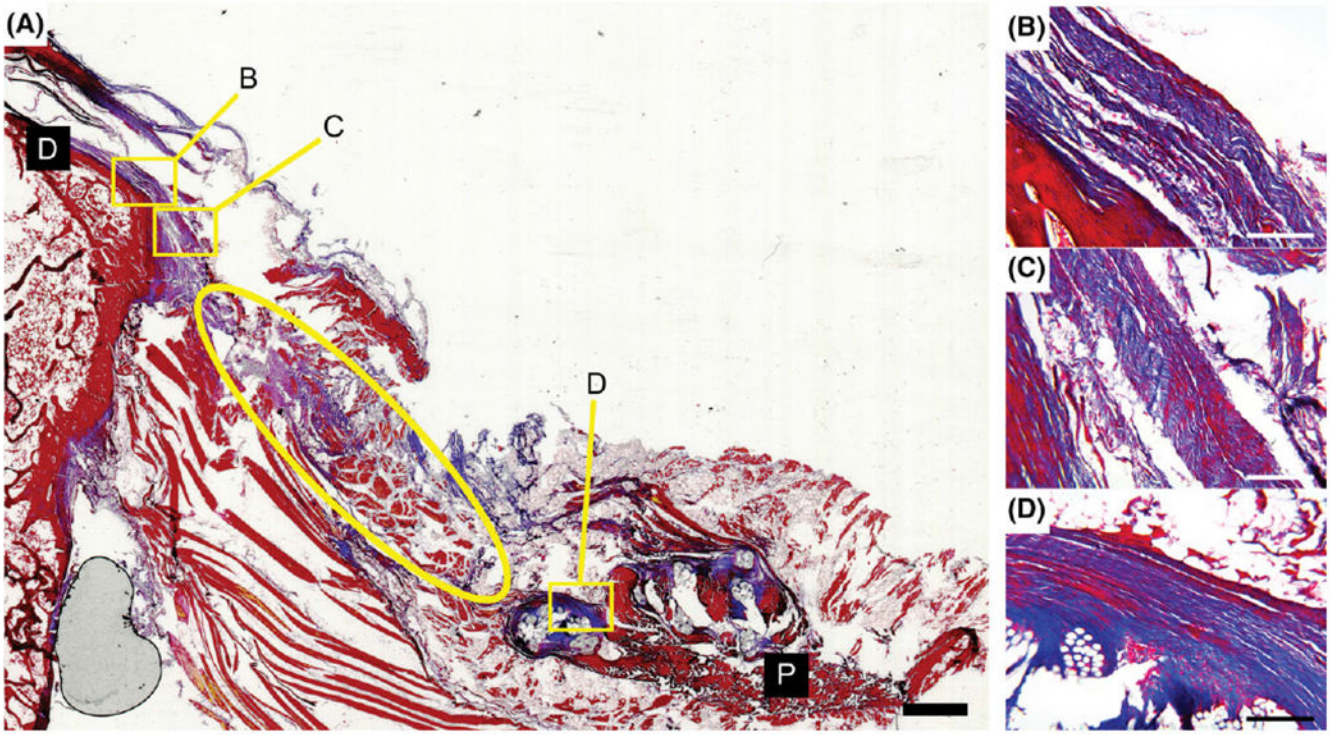

FIGURE 5.

Specimen from direct repair group stained with Masson's trichrome. Some aligned collagen deposition is seen near the surface of the bone (B and C). However, a gap appeared to form between the bone and original tendon (ellipse in A) and is potentially the result of tendon retraction during 3 months *in vivo* following the repair. Distal and proximal ends of the section are denoted by black boxes (D and P). Scale bar = 2 mm (A) and 200 μm (B–D).

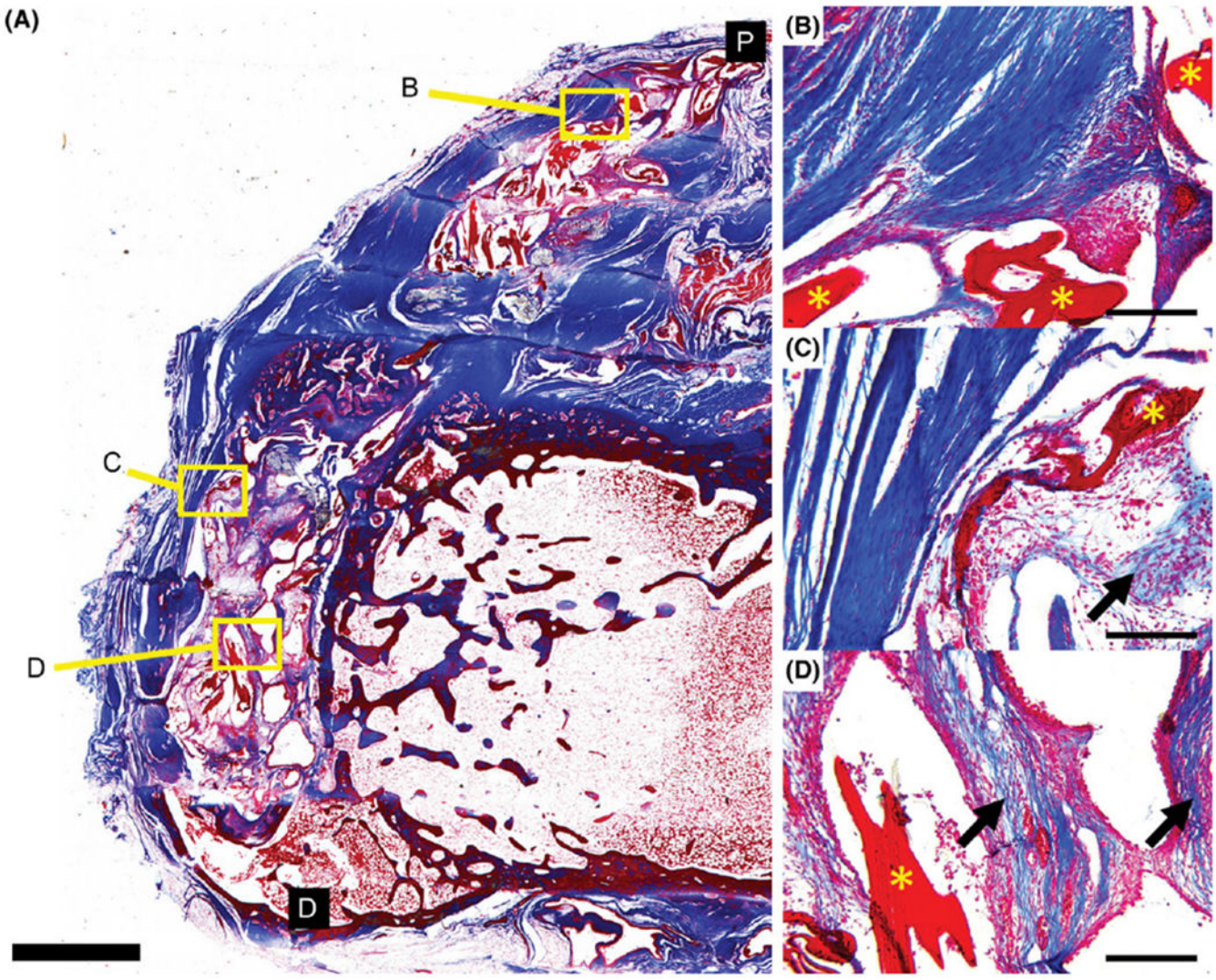

FIGURE 6.

Specimen from scaffold-alone group stained with Masson's trichrome. ELAC fibers of the scaffold are visible (*, B–D) with newly deposited collagen within the fibrous tissue immediately outside of the scaffold (arrows, B and C) as well as within the continuum of the scaffold (D). Distal and proximal ends of the section are denoted by black boxes (D and P). Scale bar = 2 mm (A) and 200 μm (B–D).

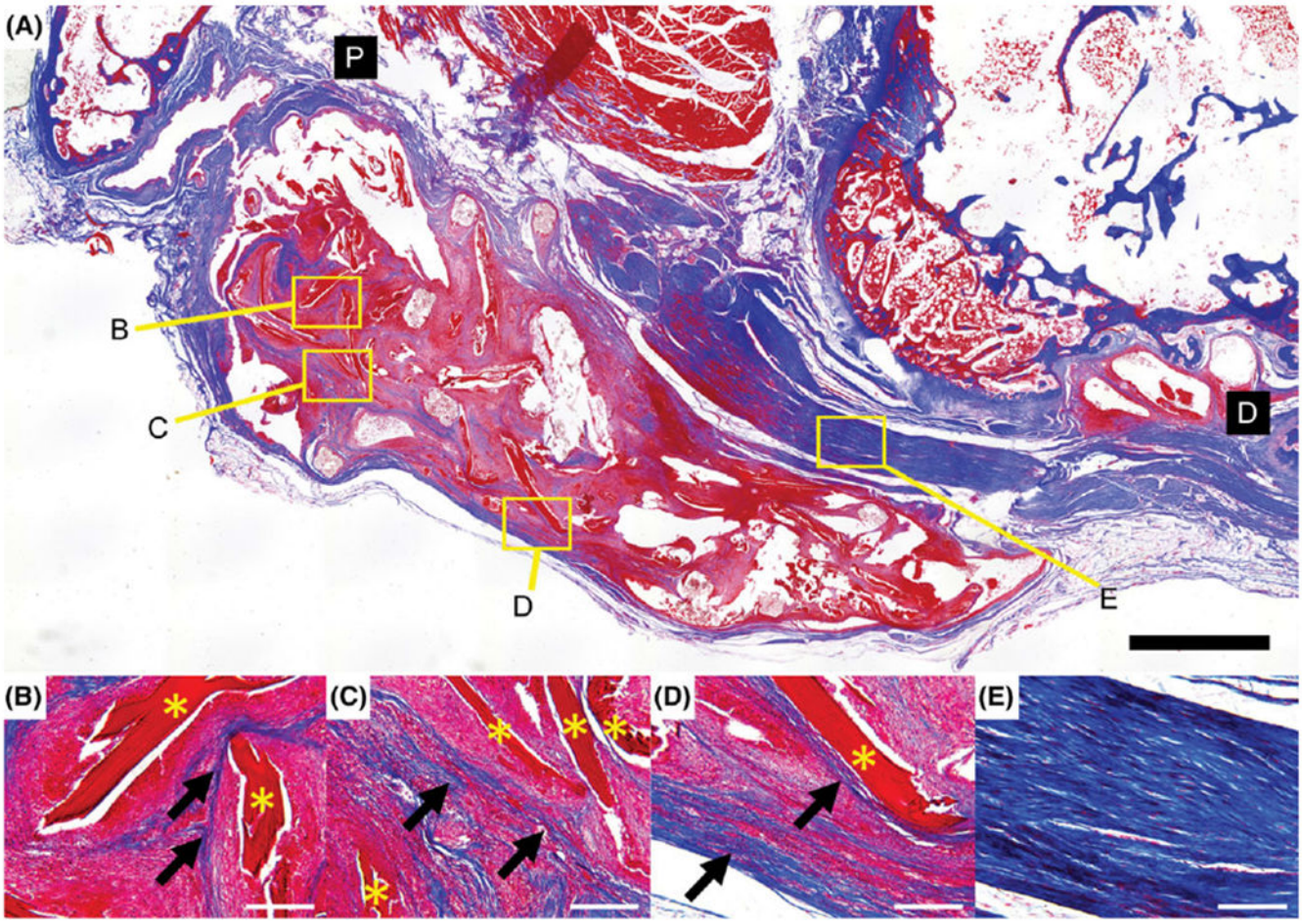

FIGURE 7.

Specimen from cell-seeded scaffold group stained with Masson's trichrome. Newly deposited collagen is visible within the continuum of the scaffold (arrows) following the contours of the ELAC fibers (*) (B–D). Extensive alignment of the collagen within the fibrous tissue surrounding the scaffold is also shown (E). Distal and proximal ends of the section are denoted by black boxes (D and P). Scale bar = 2 mm (A) and 200 μm (B–E).

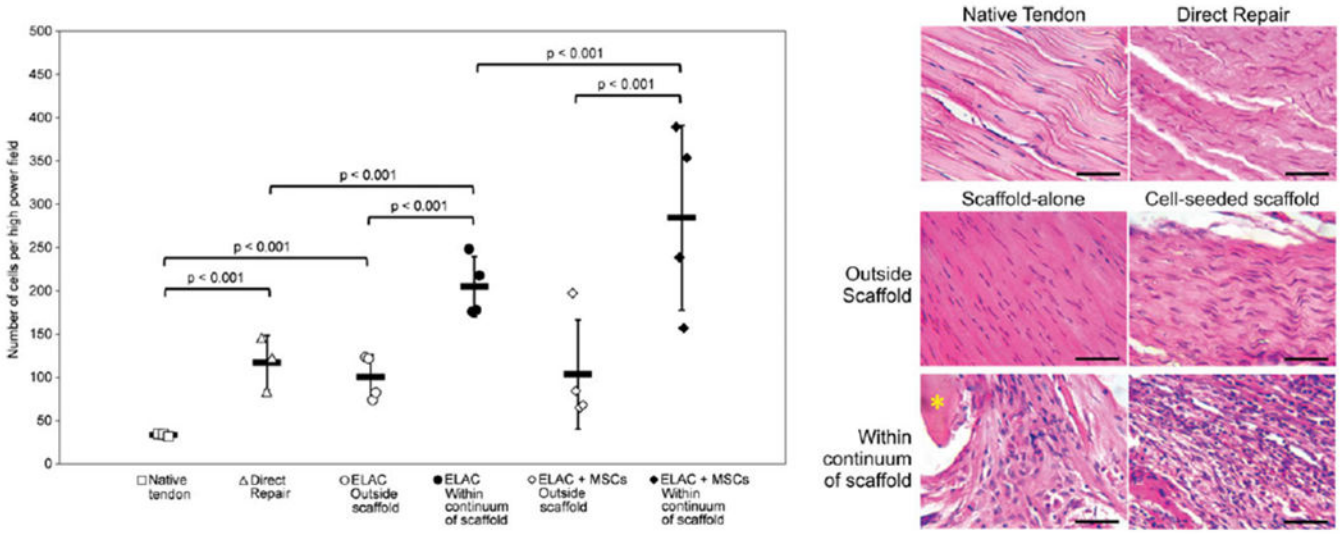

FIGURE 8.

Cells counted per HPF highlighted an increase in cellularity for all groups in comparison to native tendon (A). Error bars indicate standard error of the means. Representative specimens from each group (B) demonstrate the differences between groups in terms of cell structure, orientation, and quantity. ELAC fibers are marked with an asterisk (*). Scale bar = 50 μm.

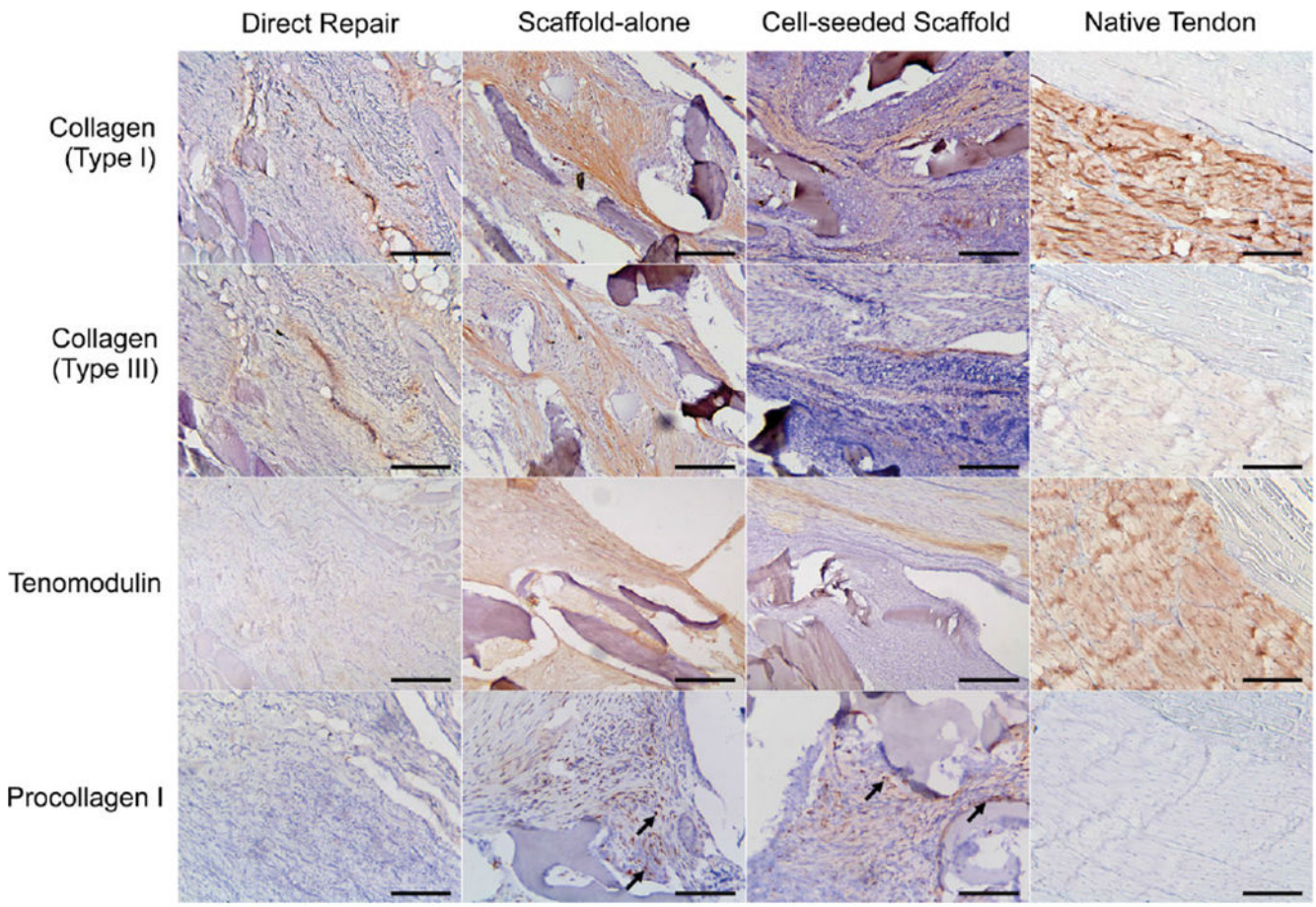

FIGURE 9.

IHC results for staining collagen I, collagen III, procollagen I, and tenomodulin. ELAC fibers are marked with an asterisk (*). Scale bar = 200 μm.

TABLE I.

Histological Scoring Table

Group	Collagen fiber structure	Collagen fiber arrangement	Rounding of nuclei	Cell population	Chronic inflammation	Total
DR	0.0	0.0	3.0 ± 0.0	1.3 ± 0.4	0.0	4.3 ± 0.4
ELAC	1.8 ± 0.2	1.6 ± 0.1	1.1 ± 0.1	1.7 ± 0.2	0.4 ± 0.2	6.6 ± 0.6
ELAC + MSCs	1.7 ± 0.1	1.2 ± 0.1	0.0	2.7 ± 0.1	0.0	5.5 ± 0.3

Native tendon parameters were defined as follows: collagen fiber structure: compact and wavy collagen fibers arranged in parallel; collagen fiber arrangement: uniaxial, an angle of less than 20° between fibers; rounding of nuclei: over 95% of nuclei predominately elongated; cell population: sparse, less than 5% coverage of the total visible area: chronic inflammation: no inflammatory cell infiltrates.

Scoring for each parameter reported as mean and standard deviation of each group. Scores were given on a scale from 0 to 3; 0 = characteristic nearly indistinguishable from native tendon, 1 = minimal difference from native tendon, 2 = moderate difference, and 3 = extensive difference. “Total” is the sum of the scoring parameters (15 = no visible characteristics of native tendon and 0 = nearly indistinguishable from native tendon).

J Biomed Mater Res B Appl Biomater. Author manuscript; available in PMC 2020 July 19.

TABLE II.

Qualitative IHC Assessment

		Scaffold alone		Cell-seeded scaffold		
	Direct repair	**Inside**	**Outside**	**Inside**	**Outside**	**Native tendon**
Collagen I	2/3	3/3	3/3	3/3	3/3	2/2
Collagen III	3/3	3/3	3/3	3/3	3/3	0/2
Tenomodulin	0/3	2/3	3/3	1/3	3/3	2/2
Procollagen I	0/3	3/3	2/3	3/3	2/3	0/2

Slides from three specimens in each of the experimental groups were assessed in a binary fashion (positive = 1, negative = 0). “Inside” refers to tissue and cells within the continuum of the scaffold structure and “outside” is in reference to the fibrous tissue immediately beyond the continuum of the scaffolds.